Article

Chemistry & Biology

Three Redundant Synthetases Secure Redox-Active Pigment Production in the Basidiomycete *Paxillus involutus*

Graphical Abstract

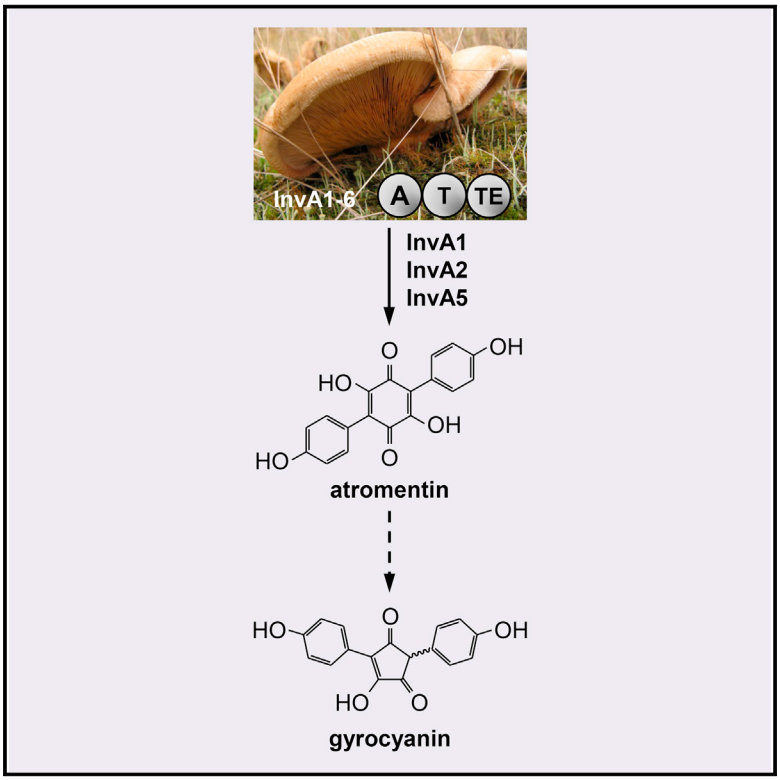

Highlights

- Diarylcyclopentenone biosynthesis proceeds via atromentin as precursor
- Atromentin biosynthesis in *Paxillus involutus* is a parallelized process
- A thioesterase signature sequence indicative for quinone formation was identified
- Quinone synthetases are amenable to engineering by domain swaps

Authors

Jana Braesel, Sebastian Götze, Firoz Shah, ..., Anders Tunlid, Pierre Stallforth, Dirk Hoffmeister

Correspondence

dirk.hoffmeister@hki-jena.de

In Brief

Diarylcyclopentenones, produced by the symbiotic fungus *Paxillus involutus*, are redox-active metabolites involved in carbon cycling as they serve Fenton-based decomposition of lignocellulose in forest ecosystems. Braesel et al. show that the fungus uses three enzymes in parallel to secure the key step in diarylcyclopentenone biosynthesis.

Braesel et al., 2015, Chemistry & Biology *22*, 1325–1334
October 22, 2015
http://dx.doi.org/10.1016/j.chembiol.2015.08.016

Chemistry & Biology
Article

Three Redundant Synthetases Secure Redox-Active Pigment Production in the Basidiomycete *Paxillus involutus*

Jana Braesel,[1] Sebastian Götze,[2] Firoz Shah,[3] Daniel Heine,[4] James Tauber,[1] Christian Hertweck,[4] Anders Tunlid,[3] Pierre Stallforth,[2] and Dirk Hoffmeister[1,*]
[1]Department of Pharmaceutical Microbiology, Hans Knöll Institute, Friedrich-Schiller-University Jena, Beutenbergstrasse 11a, 07745 Jena, Germany
[2]Junior Group Chemistry of Microbial Communication, Leibniz Institute for Natural Product Research and Infection Biology, Hans Knöll Institute, Beutenbergstrasse 11a, 07745 Jena, Germany
[3]Department of Biology, Lund University, Sölvegatan 37, 221 00 Lund, Sweden
[4]Department of Biomolecular Chemistry, Leibniz Institute for Natural Product Research and Infection Biology, Hans Knöll Institute, Beutenbergstrasse 11a, 07745 Jena, Germany
*Correspondence: dirk.hoffmeister@hki-jena.de
http://dx.doi.org/10.1016/j.chembiol.2015.08.016

SUMMARY

The symbiotic fungus *Paxillus involutus* serves a critical role in maintaining forest ecosystems, which are carbon sinks of global importance. *P. involutus* produces involutin and other 2,5-diarylcyclopentenone pigments that presumably assist in the oxidative degradation of lignocellulose via Fenton chemistry. Their precise biosynthetic pathways, however, remain obscure. Using a combination of biochemical, genetic, and transcriptomic analyses, in addition to stable-isotope labeling with synthetic precursors, we show that atromentin is the key intermediate. Atromentin is made by tridomain synthetases of high similarity: InvA1, InvA2, and InvA5. An inactive atromentin synthetase, InvA3, gained activity after a domain swap that replaced its native thioesterase domain with that of InvA5. The found degree of multiplex biosynthetic capacity is unprecedented with fungi, and highlights the great importance of the metabolite for the producer.

INTRODUCTION

The basidiomycete model fungus *Paxillus involutus* (poison pax mushroom, *Boletales*) displays a Janus-faced existence. It can cause a deadly hemolytic autoimmune reaction, infamously known as Paxillus syndrome, upon repeated ingestion of its carpophores. On the other hand, this species is of critical ecological importance, and thus represents one of the best-studied symbiotic fungi on a molecular, physiological, and environmental level. It forms symbiotic associations, so-called ectomycorrhizae, with various trees in managed and unmanaged forests, among them dominant and both silviculturally and economically important species such as spruce, pine, birch, poplar, and beech (Wallander and Söderström, 1999). A remarkable feature of *P. involutus* and numerous other species within the *Boletales* is their capacity to synthesize brightly colored aromatic pigments. These natural products fall into various subclasses, among them the pulvinic acids and the 2,5-diarylcyclopentenones, e.g., involutin and gyrocyanin (Edwards et al., 1967; Edwards and Gill, 1973; Besl et al., 1973; Steglich et al., 1977; Figure 1). These pigments display redox activity and are assumed to play a crucial role in the reduction of Fe^{3+} during the Fenton-based decomposition of litter material by *P. involutus* (Eastwood et al., 2011; Shah, 2014). Decomposition of such material by ectomycorrhizal fungi are thought to play a key role in mobilizing nutrients embedded in recalcitrant organic matter complexes, thereby making them accessible to the host plant (Lindahl and Tunlid, 2015).

Details of the pigment biosynthesis have been profoundly studied on a chemical level (reviewed by Gill and Steglich, 1987 and Zhou and Liu, 2010). Stable-isotope labeling confirmed L-tyrosine as the metabolic origin and that the terphenylquinone atromentin (Figure 1) is the direct precursor of the pulvinic acids (Hermann, 1980; Gill and Steglich, 1987). However, the biogenesis of 2,5-diarylcyclopentenones has remained enigmatic, as two routes are conceivable that either include an atromentin-independent direct condensation of 4-hydroxyphenylpyruvic acid (Figure 1, route 1) or involve atromentin formation (route 2), which then undergoes oxidative ring contraction or conversion to atromentic acid to form the cyclopentenone skeleton.

Here, we report on the biosynthesis of diarylcyclopentenone pigments in *P. involutus* and show that atromentin is their metabolic precursor, which is biosynthesized in a multiplexed process. Evidence comes from (1) in vitro characterization of six wild-type and two artificially created chimeric quinone synthetases, (2) transcriptomic data, and (3) stable-isotope labeling to track the turnover of precursors by *P. involutus*. The chimeric quinone synthetases demonstrate that successful engineering of these enzymes by replacing an entire domain is feasible. We also characterized the *P. involutus* phosphopantetheinyl transferase PptA, which converts the above quinone synthetases from the inactive *apo* into their functional *holo* forms.

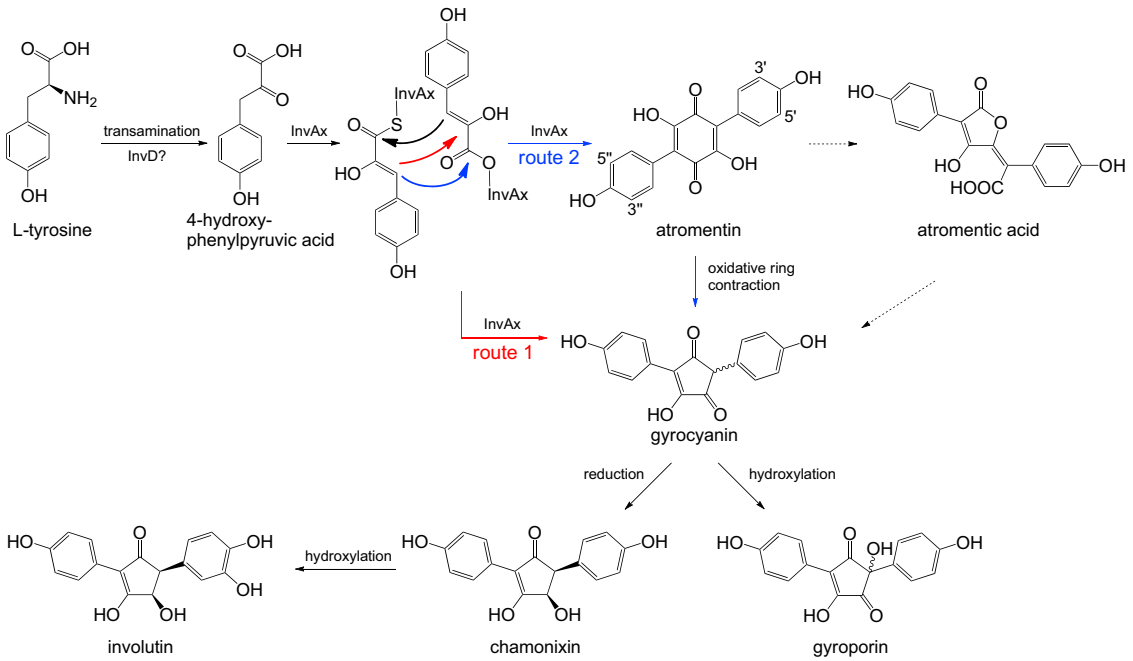

Figure 1. L-Tyrosine-Derived *Paxillus* Pigments

Schematic of pigment biosynthesis. L-Tyrosine is deaminated to 4-hydroxyphenylpyruvic acid by a PLP-dependent transaminase, followed by covalent tethering as a thioester and oxoester onto the thiolation and thioesterase domains, respectively, of the InvAx synthetases (x = 1, 2, 5). Two alternative theoretical routes may complete cyclopentenone biosynthesis. Route 1 (red) includes direct decarboxylative condensation (black and red arrows between 4-hydroxyphenylpyruvic acid units) into gyrocyanin, i.e., the common diarylcyclopentenone intermediate. Experimentally verified route 2 (blue) involves symmetric condensation (black and blue arrows between 4-hydroxyphenylpyruvic acid units) into atromentin, followed by oxidative ring contraction to yield gyrocyanin. Dotted arrows indicate a possible shunt within route 2 via atromentic acid.

RESULTS AND DISCUSSION

Genetic and Transcriptional Characterization of *invA* Genes

Diarylcyclopentenone natural products originate from the shikimic acid pathway that is likely extended by an AtrD-like transaminase activity (Schneider et al., 2008) to produce 4-hydroxyphenylpyruvic acid from L-tyrosine. However, the mechanistic basis for the condensation of two 4-hydroxyphenylpyruvic acid units into the diarylcyclopentenone scaffold has remained obscure. Two routes appear plausible (Figure 1, routes 1 and 2), which either require or bypass atromentin as a precursor. In the atromentin-dependent scenario that requires atromentin synthetase activity (route 2), atromentin may undergo oxidative ring contraction to yield the cyclopentenone scaffold in a one-step process, or is converted into atromentic acid, i.e., a butenolide, which then serves as intermediate for cyclopentenone formation (Gill and Steglich, 1987). An alternative biosynthetic scenario (route 1) includes a direct condensation of 4-hydroxyphenylpyruvate (Gruber et al., 2014), thereby bypassing an atromentin intermediate but still requiring enzymatic activation, most likely through adenylate formation. To shed more light onto the biogenesis of fungal diarylcyclopentenones, we searched the genome of the basidiomycete *P. involutus* ATCC 200175 (Kohler et al., 2015) for genes encoding adenylating multidomain enzymes, as they were shown to catalyze formation of carbon-carbon or carbon-oxygen bonds between aromatic α-keto acid building blocks (Schneider et al., 2008; Wackler et al., 2012). Six candidate genes were identified, hereafter referred to as *invA1* to *invA6* (Figure 2A). These genes encode putative tridomain monomodular synthetases, each featuring an adenylation (A), a thiolation (T), and a thioesterase (TE) domain (Figure 2B). The signature motifs of these domains followed the established consensus (Schwarzer et al., 2003). InvA1–A6 are 955, 953, 949, 950, 953, and 952 amino acids long, respectively, with theoretical molecular masses of 104.8, 104.6, 104.4, 105.0, 104.6, and 104.7 kDa. The sequences shared 74%–83% identical amino acids with the *Suillus grevillei* atromentin synthetase GreA (protein accession NCBI: AFB76152.1), and 67%–76% with the *Tapinella panuoides* atromentin synthetase AtrA (ACH 90386.1). The Joint Genome Institute protein IDs for InvA1–A6 are JGI: 166672, 69019, 127833, 127875, 77684, and 69028, respectively.

The gene *invA5* is located on scaffold 16 of the *P. involutus* genome, while all other *invA* genes are encoded on scaffold 4 (Figure 2A). The *invA2* and *invA3* genes are encoded in the vicinity of a putative aminotransferase gene, which is referred to as *invD*. It is hypothesized to encode the gateway enzyme for terphenylquinone/atromentin biosynthesis, as other highly similar fungal enzymes, TdiD and AtrD, were shown to be responsible for the first step in bis-indolylquinone and terphenylquinone formation (Schneider et al., 2007, 2008). Scaffold 4 also encodes other genes that are potentially involved in secondary metabolism, encoding four transporters of the major facilitator

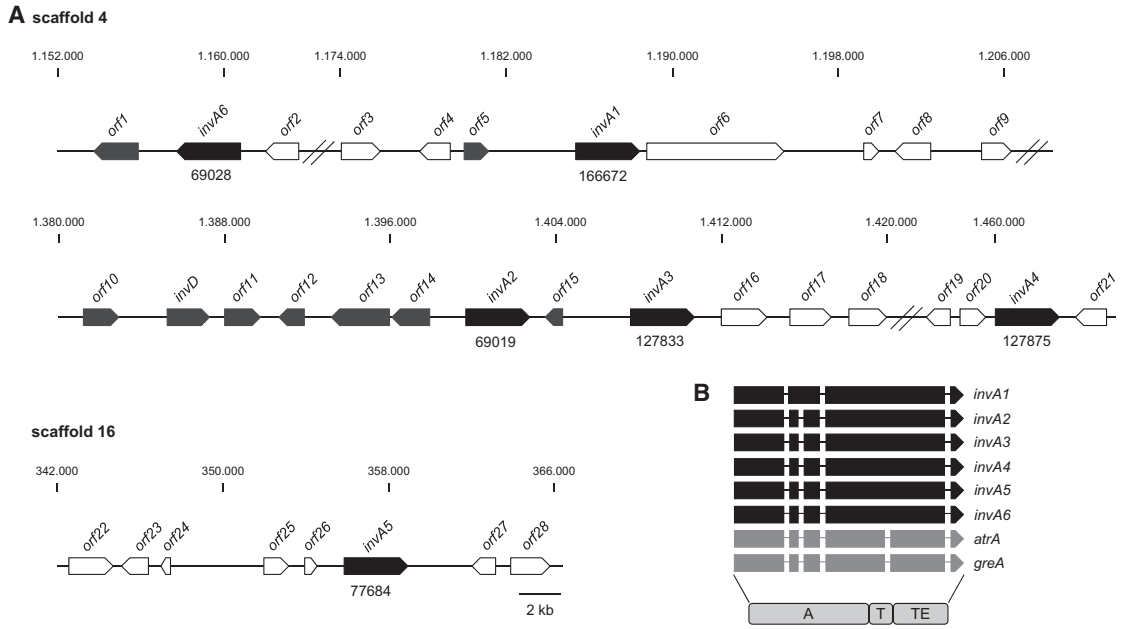

Figure 2. Physical Map of Biosynthetic Genes and Synthetase Gene Structures

(A) Genes *invA1-invA6* (black arrows) and adjacent reading frames are located on scaffolds 4 and 16 in the genome of *P. involutus*. Open arrows represent hypothetical reading frames; gray arrows represent putative transporter and biosynthesis genes. Protein IDs for InvA1 to InvA6 are indicated below the respective arrows, and base counts of the scaffolds are indicated above the genes. For clarity, introns are not shown.

(B) Comparison of the structures of *P. involutus* synthetase genes *invA1–A6* (black) and basidiomycete orthologs *atrA* of *Tapinella panuoides* and *greA* of *Suillus grevillei* (gray). Lines represent introns. The domain setup of InvA1–A6, AtrA, and GreA is shown below the genes. A, adenylation domain; T, thiolation domain; TE, thioesterase domain.

superfamily (*orf11*, *orf13–orf15*), an oxidoreductase (*orf1*), a glycosyltransferase (*orf5*), an aldo-keto reductase (*orf10*), and an alcohol dehydrogenase (*orf12*).

Transcriptomic analysis identified *invA1* to *invA6* as expressed genes, when the fungus is grown in axenic culture, regardless of the media tested. Analysis of relative transcript levels showed a high abundance of *invA1*, *invA2*, and *invA5* transcripts, and moderate levels of *invA6* mRNA. In contrast, *invA3* and *invA4* were only poorly expressed. When using media containing organic nitrogen, we found a more than 13-fold and 15-fold higher number of transcripts encoding *invA1* and *invA5*, respectively, compared with *invA3* or *invA4*. The transcripts of *invA1* and *invA5* were about 5-fold more abundant than those of *invA6*, and 1.4-fold and 2-fold higher compared with *invA2*. The experimentally verified cDNA sequences for *invA1* and *invA3* deviate from the predicted sequences deposited on the JGI server. For these genes, additional 673- and 595-bp introns, respectively, were erroneously predicted in the center portion of the reading frame. By amplification of partial sequences of genomic and cDNA, we showed that the protein sequence of InvA3 is one amino acid shorter than predicted.

The genes *invA1* possesses three and *invA2–A6* four introns, which are between 50 and 61 bp in length (Figure 2B). The intron positions are conserved in the *invA* orthologs *atrA* and *greA*. However, these genes are interrupted by a fifth intron in their 3′-terminal portions. For *invA3* and *invA6*, erroneously spliced transcripts were found that either included retained introns or erroneously removed exonic sequences. The resulting shifted reading frames lead to premature stop codons and, consequently, non-functional proteins. Transcript variants of a gene may be interpreted as a posttranscriptional regulatory mechanism (Conti and Izaurralde, 2005) and are also described for the basidiomycetes *Phanerochaete chrysosporium* and *Armillaria mellea* (Larrondo et al., 2004; Misiek and Hoffmeister, 2008).

P. involutus 4′-Phosphopantetheinyl Transferase

For enzymatic activity, multidomain biosynthesis enzymes, such as peptide and quinone synthetases, strictly require posttranslational modification by 4′-phosphopantetheinyl (4′-PPT) transfer to a conserved serine residue within the T domain. This 4′-PPT transfer is catalyzed by dedicated transferases (so-called Sfp-type 4′-PPTase). As no such enzyme of basidiomycete origin has yet been described or characterized, we carried out a tblastn search across the *P. involutus* genome, using the sequence of *Aspergillus nidulans* 4′-PPTase NpgA (Keszenman-Pereyra et al., 2003) as query. A gene encoding a 263-amino-acid putative Sfp-type 4′-PPTase (OMIM: 174503) was identified on scaffold 3 of the *P. involutus* genome. The 1,004-bp gene includes four introns and is referred to as *pptA* hereafter. PptA shares 54% identical amino acids with a predicted 4′-phosphopantetheinyl transferase of *Gloeophyllum trabeum* ATCC 11539 (accession number NCBI: XP_007861898).

Biochemical Characterization of Putative Synthetases

The *apo*-proteins InvA1–A6 were heterologously produced in *Escherichia coli* KRX and SoluBL as N-terminally hexahistidine-tagged fusion proteins (Figure S1). Substrate specificity, temperature, and pH optima of the A domains of *apo*-InvA1–A6 were

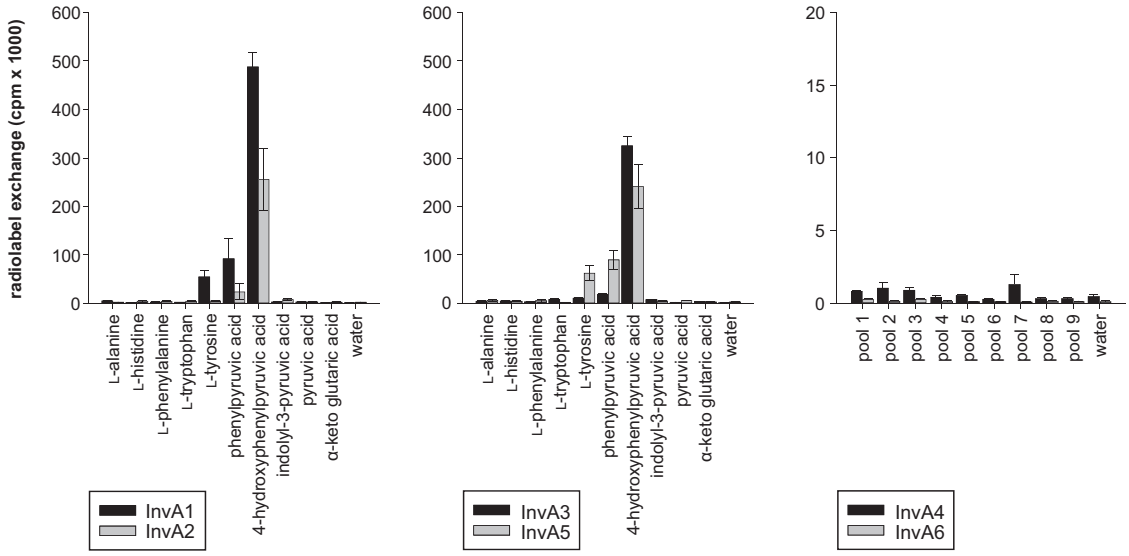

Figure 3. Substrate Specificity of the Adenylation Domains InvA1 to InvA6

Substrate specificity was determined in vitro using the substrate-dependent ATP-[^{32}P]pyrophosphate exchange assay. Error bars indicate SD. Left: InvA1 and InvA2; center: InvA3 and InvA5; right: InvA4 and InvA6. The latter enzymes were tested with 37 substrates, combined in nine pools (Table S2). Polyacrylamide gels of purified proteins and initial substrate screens are shown in Figure S1.

characterized using the ATP-[^{32}P]pyrophosphate radiolabel exchange assay.

As *Paxillus* pigments originate from the shikimic acid pathway, aromatic 2-oxo acids and aromatic L-amino acids were tested as potential substrates, along with pyruvic acid and L-alanine as controls. Strongest pyrophosphate exchange by InvA1–A3 and InvA5 was observed with 4-hydroxyphenylpyruvic acid (InvA1: 487,600 cpm; InvA2: 255,600 cpm; InvA3: 325,200 cpm; InvA5: 241,100 cpm; Figure 3). 4-Hydroxyphenylpyruvic acid is the expected initial building block for diarylcyclopentenones, irrespective of the biosynthetic route. With the pyrophosphate exchange normalized with respect to 4-hydroxyphenylpyruvic acid, phenylpyruvic acid was turned over between 5.8% and 37.4%, and L-tyrosine between 2.1% and 26%, respectively. However, these compounds and a subsequently tested extended set of potential substrates, i.e., pools comprising 37 compounds (L-amino acids, α-keto acids, and aromatic carboxylic acids, Table S2) were rejected by InvA4 and InvA6 (<2,000 cpm; Figures 3 and S1). Therefore, their substrate preferences remain unknown but are incongruent with those of the other tested InvA enzymes. Alternatively, InvA4 and InvA6 may have lost enzymatic activity. Crystallography and biochemical evidence have established ten key amino acid residues within the primary amino acid sequence of A domains that are most likely involved in substrate recognition (Stachelhaus et al., 1999). This sequence signature, also referred to as non-ribosomal code, of the InvA enzymes is V-A-E-F-S-G-G-A-C-K, except for InvA4, whose signature bears a glycine instead of a glutamic acid at the third position (V-A-G-F-S-G-G-A-C-K). This signature is conserved in the biochemically characterized atromentin synthetases AtrA and GreA (Schneider et al., 2008; Wackler et al., 2012). Therefore, our biochemical results confirm this signature as specific non-ribosomal code for aromatic α-keto acid-activating synthetases. Optimal pyrophosphate exchange with InvA1–A3 and InvA5 took place at 20°C (InvA2, InvA3) and 25°C (InvA1, InvA5), and at pH 7.2, 7.6, 6.8, 7.4 for InvA1, InvA2, InvA3, and InvA5, respectively.

InvA1–A3 and InvA5 were treated in vitro with the heterologously produced 4′-PPTases Svp (Sanchez et al., 2001) and, in separate reactions, with *P. involutus* PptA (Figure S1), to produce the *holo*-enzyme. *Holo*-InvA enzymes were separately incubated with 1.8 mM 4-hydroxyphenylpyruvic acid under optimum conditions in Mg^{2+}-containing Tris buffer and 2.5 mM ATP. After 16 hr of incubation, the reactions containing InvA1, InvA2, and InvA5, respectively, turned violet, irrespective of the 4′-PPTase used for priming.

In negative controls without ATP or a 4′-PPTase, this coloration was not observed. The UV-visible spectrum, high-resolution mass (found *m/z* 323.0555 $[M - H]^-$, calculated for $C_{18}H_{12}O_6$: *m/z* 323.0561 $[M - H]^-$), and retention time of the colored compound were identical to an authentic atromentin sample (Figure 4). We therefore conclude that InvA1, InvA2, and InvA5 are atromentin synthetases, which is consistent with earlier reports that *P. involutus* does have the capacity to produce atromentin (Bresinsky and Rennschmidt, 1971; Bresinsky, 1974).

Usually, fungi rely on one set of small-molecule biosynthetic pathway genes per haploid genome. A three-fold redundantly secured natural product biosynthesis pathway is unprecedented with fungi, but points to an indispensable ecological role of the diarylcyclopentenone products, likely to degrade organic matter in forest ecosystems. This feature is somewhat reminiscent of a duplicated cluster of genes in *Aspergillus flavus*, which encode the production of the same set of piperazines that are essential for sclerotia formation (Forseth et al., 2013).

Product formation was not observed with InvA3, whereas the ATP-[^{32}P]pyrophosphate exchange assay verified that the A domain is active and adenylates 4-hydroxyphenylpyruvic acid. Therefore, we hypothesized that the TE domain that would

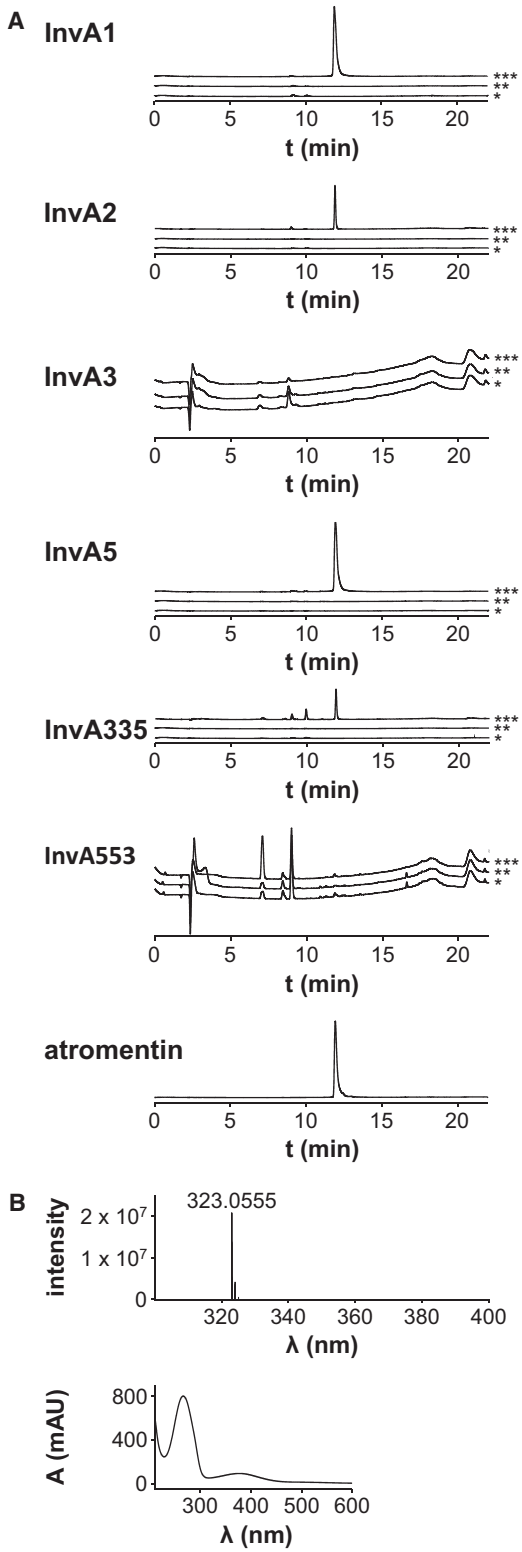

Figure 4. Chromatographic Analysis of InvA-Mediated In Vitro Synthesis of Atromentin by PptA-Primed Synthetases

(A) Enzymatic reactions and authentic atromentin standard. Single asterisk indicates control without ATP, double asterisk control without PPTase, and triple asterisk the reaction. Absorption of the signal at t_R = 11.9 min is: InvA1, 661 mAU; InvA2, 394 mAU; InvA5, 635 mAU; InvA335, 258 mAU; standard, 745 mAU. The signals at t_R = 9.0 and 9.5 min represent unconverted substrates. Maximum absorption in InvA3 and InvA553 chromatograms was <20 mAU; for all other chromatograms the maximum absorption was 800 mAU.

(B) High-resolution mass spectrometry profile and UV-visible spectrum of authentic atromentin. These spectra were also found in enzymatic reactions. Detection wavelength was λ = 254 nm.

catalyze symmetric condensation of two 4-hydroxyphenylpyruvic acid units into a substituted benzoquinone may be inactive. Furthermore, we assumed that replacing the InvA3 TE domain by a TE domain of an active *P. involutus* atromentin synthetase might reconstitute its functionality. To test this hypothesis, we constructed a chimeric gene (*invA*335) that encoded the InvA3 A-T didomain fused to the InvA5 TE domain. For negative control, we also created the inverse chimera, termed *invA*553, encoding a synthetase composed of the InvA5 A-T didomain and the InvA3 TE domain. For product formation, either chimera was heterologously produced as hexahistidine fusion in *E. coli* (for SDS gel picture, see Figure S1), converted in vitro into the *holo* form by 4′-PPTases Svp or PptA, and incubated under optimum conditions, as described above.

High-performance liquid chromatography (HPLC) analysis clearly showed atromentin production in vitro by the chimera InvA335, whereas the chimeric synthetase InvA553 did not produce atromentin, or any other compound, in detectable amounts (Figure 4). This result demonstrates that the wild-type InvA3 enzyme is inactive because of its non-functional TE domain, and gains full functionality when the TE domain is replaced. Engineering of quinone synthetases has not been reported as yet. Our results demonstrate that they are amenable to domain swaps. This finding may open up new avenues of research to engineer multimodular enzymes, as quinone synthetases represent a simple model for the study of interdomain interactions that involve TE domains.

Signature Sequence of Quinone-Forming Thioesterase Domains

Numerous non-ribosomal peptide synthetases (NRPSs) rely on a TE domain for product release (Schwarzer et al., 2003). Crystallographic analysis of the surfactin A synthetase SrfA-C and bioinformatics analyses revealed that TE domains belong to the α/β-hydrolase superfamily (Bruner et al., 2002; Samel et al., 2006; Cantu et al., 2010). The TE domain catalytic triad is composed of the residues Ser80, Asp107, and His207 (numbering according to Bruner et al., 2002). The InvA synthetases show strictly conserved serine and histidine residues, with the second residue of the triad being variable (Table 1). InvA3, InvA4, and InvA6 harbor the conserved aspartate residue. In those enzymes that showed quinone synthetase activity, i.e., InvA1, InvA2, and InvA5, this residue was replaced by an asparagine (Table 1). We compared the sequences of all characterized quinone and furanone synthetases available from the literature, which include NPS3, TdiA, AtrA, GreA, BthII0204, EchA, RalA, and MicA (Eastwood et al., 2011; Schneider et al., 2007, 2008; Wackler et al., 2011, 2012; Biggins et al., 2011; Zhu et al., 2014; Yeh et al., 2012), along with TE domains of multimodular NRPSs, and identified a dichotomous motif pattern. Quinone synthetases, including InvA1, InvA2, and InvA5, consistently

Table 1. Catalytic Triads of InvA1–A6, Other NRPS-like Enzymes, and NRPSs, Based on Alignment of Their TE Domains with GENEIOUS Software, Version 7.1.4, Using SrfTE as Reference

Protein	Species	Catalytic Triad[a]																				Product	Protein Accession #/NCBI Reference
InvA3	*Paxillus involutus*	G	Y	**S**	Y	G	…	V	I	**D**	-	-	-	I	I	…	G	H	**H**	Y	T	unknown	127833
InvA4	*Paxillus involutus*	G	Y	**S**	Y	G	…	I	I	**D**	-	-	-	M	I	…	G	H	**H**	Y	T		127875
InvA6	*Paxillus involutus*	G	Y	**S**	Y	G	…	L	V	**D**	I	P	P	H	I	…	G	H	**H**	D	T		69028
InvA1	*Paxillus involutus*	G	Y	**S**	Y	G	…	L	I	**N**	I	P	P	H	I	…	G	Q	**H**	Y	T	quinone	166672
InvA2	*Paxillus involutus*	G	Y	**S**	Y	G	…	L	I	**N**	I	P	P	H	I	…	G	Q	**H**	Y	T		69019
InvA5	*Paxillus involutus*	G	Y	**S**	Y	G	…	L	I	**N**	I	P	P	N	I	…	G	Q	**H**	Y	T		77684
AtrA	*Tapinella panuoides*	G	Y	**S**	Y	G	…	L	I	**N**	I	P	P	H	I	…	G	Q	**H**	Y	T		ACH90386.1
GreA	*Suillus grevillei*	G	Y	**S**	Y	G	…	L	I	**N**	I	P	P	H	I	…	G	Q	**H**	Y	T		AFB76152
Nps3[a]	*Serpula lacrymans*	G	Y	**S**	Y	G	…	L	I	**N**	I	P	P	H	I	…	G	R	**H**	Y	T		EGO23141.1
TdiA	*Aspergillus nidulans*	G	Y	**S**	F	G	…	S	W	**N**	L	P	P	H	I	…	G	A	**H**	Y	T		CBF80711.1
BthII0204[b]	*Burkholderia pseudomallei*	G	Y	**S**	Y	G	…	S	F	**N**	L	P	P	H	I	…	G	E	**H**	Y	T		CAH37575
EchA	*Streptomyces* sp. LZ35	G	Y	**S**	Y	G	…	S	F	**N**	L	P	P	H	I	…	P	G	**H**	Y	T		YP_008789943
MicA[b]	*Aspergillus nidulans*	G	Y	**S**	L	G	…	S	I	**D**	Y	P	P	H	I	…	G	I	**H**	A	K	furanone	XP_661000.1
RalA	*Ralstonia solanacearum*	G	Y	**S**	Y	G	…	S	I	**D**	A	P	P	V	I	…	G	E	**H**	H	T		AEC03968.1
GrsB	*Bacillus brevis*	G	Y	**S**	S	G	…	L	F	**D**	V	-	-	Y	W	…	G	A	**H**	S	N	ester/ peptide	CAA43838
TycC	*Bacillus brevis*	G	Y	**S**	S	G	…	L	F	**D**	S	-	-	Y	W	…	G	I	**H**	S	R	(macro-cycles)	O30409
FenB	*Bacillus subtilis*	G	Y	**S**	A	G	…	I	V	**D**	A	-	-	Y	K	…	G	A	**H**	K	D		AAB00093.1
SrfA-C	*Bacillus subtilis*	G	Y	**S**	A	G	…	M	V	**D**	S	-	-	Y	K	…	G	T	**H**	A	E		WP_029878554

After Bruner et al. (2002).

[a]The residues of the catalytic triad Ser80, Asp107, and His207 (numbering according to SrfTE) are marked in bold.

[b]Enzymatic function deduced from indirect evidence, as these enzymes have not yet been characterized biochemically.

showed a Ser/Asn/His triad, with the asparagine being followed by a branched-chain aliphatic amino acid (leucine or isoleucine) and two proline residues. Synthetases catalyzing furanone assembly (RalA and MicA) and thioesterases of macrolacton/macrolactam forming peptide synthetases SrfTE, FenTE, TycTE, and GrsTE (Bruner et al., 2002; Samel et al., 2006; Trauger et al., 2000; Hoyer et al., 2007) showed the regular Ser/Asp/His triad (Table 1). The aspartate residue within the catalytic triad hydrogen bonds and polarizes the histidine. A recent report describes an engineered catalytic triad of a *Listeria monocytogenes* caseinolytic protease (ClpP). The authors report that substituting the naturally occurring asparagine by aspartate increased hydrolysis, favored oligomerization, and impacted on an adjacent Asp/Arg oligomerization sensor sequence (Zeiler et al., 2013) which is, however, not present in any of the aforementioned natural product TE domains. Furthermore, the presence of a sequence motif composed of an aliphatic residue and a double proline that immediately follows the asparagine seems restricted to synthetases that condense two monomers into a quinone natural product scaffold, i.e., rather small products, compared with the macrocycle-forming NRPSs. Although the functional role of the neutral asparagine, combined with the above motif, remains elusive in the context of these synthetases, it appears critical for quinone formation from aromatic α-keto acids and helps selectively recognize quinone synthetases. Notably, the inactive *Paxillus* synthetases, InvA3 and InvA4, lack the double proline motif (Table 1). InvA6 is also inactive and also shows an aspartic acid residue, like InvA3 and InvA4, but has the Ile-Pro-Pro motif. A chimeric enzyme, encoded by the *invA*556 gene and comprising the InvA5 A-T didomain fused to the InvA6 TE domain, was used to test whether the InvA6 thioesterase is functional. InvA556 adenylated 4-hydroxyphenylpyruvic acid but did show product formation (data not shown). We therefore conclude that the adenylation and thioesterase domains of InvA6 are inactive. Taken together, these findings support our in vitro data of InvA3, InvA4, and InvA6 as not being relevant for atromentin production.

Stable-Isotope Labeling

InvA1, InvA2, and InvA5 were shown to possess atromentin synthetase activity, while InvA3 turned functional only after artificially replacing its TE domain, probably because of the aforementioned deviating TE motifs. InvA4 and InvA6 did not accept 4-hydroxyphenylpyruvic acid. Hence, InvA3, InvA4, and InvA6 could be excluded as not being relevant for biosynthesis of 2,5-diarylcyclopentenone or their likely biosynthetic precursor atromentin. However, we could still not discount a scenario of direct cyclopentenone formation by any of these enzymes in vivo via route 1 (Figure 1), thereby altogether bypassing atromentin as intermediate. Therefore, we carried out feeding experiments with stable-isotope-labeled atromentin, followed by HPLC and mass spectrometry analysis. When 3′,3″,5′,5″-D_4-atromentin was administered to the homogenized mycelium, the deuterium label clearly appeared in two cyclopentenones, gyrocyanin and its oxidation product gyroporin (Figure 5), whose masses were found to increase by four mass units (gyrocyanin: *m/z* 295.0615; D_4-gyrocyanin: *m/z* 299.0861; gyroporin: *m/z* 311.0558; D_4-gyroporin: *m/z* 315.0813 $[M - H]^-$), thereby demonstrating that atromentin serves as cyclopentenone precursor. Gyrocyanin was identified by comparison of

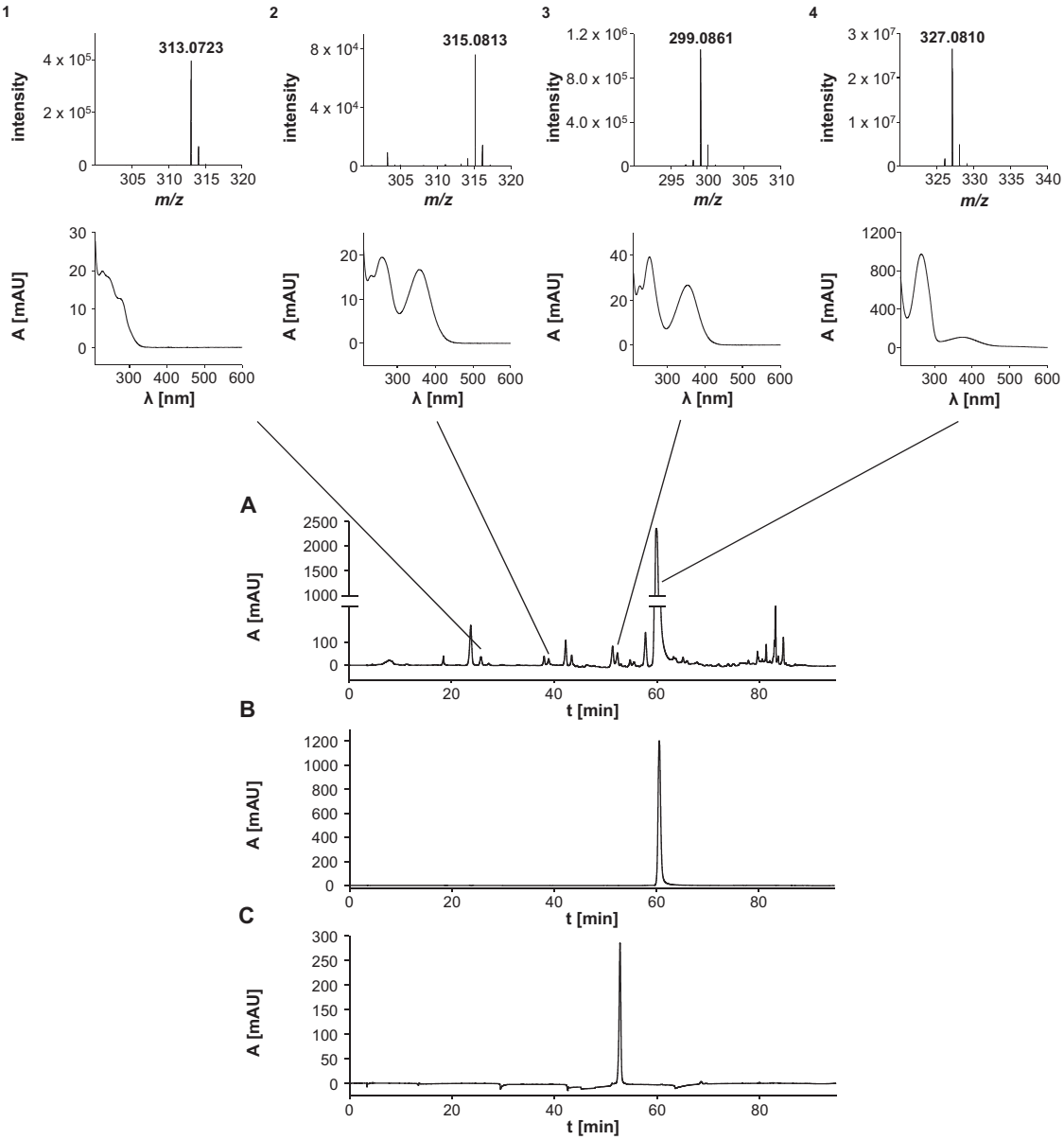

Figure 5. Chromatographic Analysis of the Isotope-Labeling Experiment

(A) Tetradeuterated atromentin, added to *P. involutus* mycelial homogenate.

(B and C) Authentic atromentin (B) and synthetic gyrocyanin (C). Chromatographic signals: t_R = 25.7 min for involutin (compound 1); t_R = 38.9 min for gyroporin (2); t_R = 52.3 min for gyrocyanin (3); t_R = 60.4 min for atromentin (4). Detection wavelength was λ = 254 nm. Mass spectra of mycelial homogenate supplemented with unlabeled atromentin are shown in Figure S2.

chromatographic and mass spectrometric characteristics with a synthetic reference (see Supplemental Experimental Procedures). Involutin was found only in non-deuterated form (*m/z* 313.0723 $[M - H]^-$), likely due to the mycelial homogenate failing to reduce gyrocyanin into chamonixin (Figure 1), with the latter only being detectable in negligible traces and in non-deuterated form by mass spectrometry.

3′,3″,5′,5″-D_4-atromentin was also added to intact *P. involutus* cultures at 1.5 mM final concentration. As fungi usually secrete atromentin and/or its follow-up products out of the cells and given the competing cellular biosynthesis of non-labeled atromentin, we expected very minor quantities of deuterated atromentin being taken up and catalytically converted by the cells, and being secreted back into the medium. We therefore resorted to single-ion monitoring high-resolution electrospray ionization mass spectrometry (HRESI-MS) for analysis. The mass spectrometric data (Figure S2) supported the above findings, as they demonstrated the presence of tetradeuterated gyrocyanin and gyroporin as well. We also detected the mass (*m/z* 301.1017 $[M - H]^-$) of tetradeuterated chamonixin (Besl et al., 1980), the biosynthetic follow-up product downstream of gyrocyanin. Unlabeled involutin, which is three biosynthetic steps away from

atromentin, and atromentic acid, which is a direct follow-up product of atromentin, were present in traces (Figure S2). Our data cannot fully rule out a route involving atromentic acid, i.e., a butenolide intermediate. However, our data strongly favor the latter model, since merely traces of atromentic acid were detectable by HRESI-MS, and diarylcyclopentenone biosynthesis in *P. involutus* proceeds through the terphenylquinone atromentin. This compound represents the common intermediate of both the atromentic acid/pulvinic acid and the thelephoric acid family of fungal pigments. Our results expand its significance by adding the cyclopentenones as another atromentin-derived class of ecologically relevant basidiomycete natural products.

SIGNIFICANCE

The basidiomycete *P. involutus* represents a model organism for ectomycorrhizae. These tree-fungus symbioses are critical for functional forest ecosystems, which are carbon sinks of global importance. To mobilize nutrients embedded in forest litter material, this fungus relies on Fenton chemistry to help degrade complex organic biomass and, thus, maintain carbon cycling. This chemistry requires redox-active 2,5-diarylcyclopentenone pigments, e.g., involutin. Our study demonstrates that the biosynthetic key intermediate is the terphenylquinone atromentin, which is supplied in a parallelized physiological process. The highly and simultaneously expressed genes *invA1*, *invA2*, and *invA5* encode functional three-domain quinone synthetases to secure atromentin biosynthesis. A three-fold multiplex natural product pathway is unprecedented with fungi, yet underlines the ecological significance of environmentally relevant redox-active cyclopentenones.

EXPERIMENTAL PROCEDURES

General Procedures and Culture Conditions

P. involutus ATCC 200175 was routinely grown at 23°C as still culture on liquid modified Melin-Norkrans (MMN) medium. Molecular genetic procedures were carried out according to the manufacturers' instructions (Fermentas, NEB, Promega) or as described below. Chemicals were purchased from Alfa Aesar, Sigma-Aldrich, Roth, and VWR, except [^{32}P]pyrophosphate, which was obtained from PerkinElmer, and deuterated L-tyrosine (ring-3,5-D_2, 98%), which was purchased from Cambridge Isotope Laboratories. The genomic sequence of *P. involutus* ATCC 200175 is available through the Mycocosm genome portal at the Joint Genome Institute (Kohler et al., 2015).

Cloning of *invA1–invA6* and *pptA* cDNAs

The SV total RNA isolation system (Promega) was used to purify total RNA from *P. involutus* mycelium. First-strand synthesis was primed with a 16-mer oligo(dT)-primer (40 pmol) and carried out in the supplied buffer, with $MgCl_2$ (2 mM), dinucleotide triphosphates (dNTPs) (0.5 mM each), and ImProm reverse transcriptase, in a total volume of 20 μl. A portion of the first-strand reaction (3 μl) was used as template in subsequent PCRs. The reactions (50 μl) to amplify cDNAs of *invA1*, *invA3*, and *invA6* consisted of 3 mM $MgCl_2$, 0.2 mM each dNTP, 40 pmol (each) primer (Table S1), and 1 U Phusion DNA polymerase in the buffer supplied with the enzyme and using the following thermal cycling parameters: 30 s at 98°C; 30–35 cycles of 98°C for 10 s, 59°C–66.5°C for 20 s, and 72°C for 105 s; and a terminal hold for 5 min at 72°C. The cDNAs of genes *invA4* and *invA5* were amplified with 4 mM $MgSO_4$, 0.2 mM each dNTP, 40 pmol (each) primer (Table S1), and 1.5 U pfu DNA polymerase in the buffer supplied with the enzyme, in a total volume of 50 μl. Thermocycling conditions were initial denaturation: 2 min at 95°C; amplification: 35 cycles (95°C for 30 s, 60°C–65°C for 30 s, 72°C for 8 min); terminal hold: 10 min at 72°C. The primers introduced restriction sites into the PCR products, which were cloned into expression vectors pET28b and pRSETb, respectively, to create plasmids pJB051 (to express *invA5*), pJB064 (*invA4*), pJB078 (*invA1*), pJB080 (*invA6*), and pJB082 (*invA3*). Codon-optimized cDNAs of *invA2*, *invA3*, *invA6*, and *pptA* were synthesized by a commercial vendor (GenScript). The cDNAs of *invA2* and *pptA* were ligated to the *Nde*I and *Bam*HI sites of pET28b to create pJB053 (to express *invA2*) and pJB062 (*pptA*), respectively. The *invA6* cDNA was ligated to the *Nde*I and *Bam*HI sites of pET28b, to create plasmid pJB066, and later excised and ligated into equally cut pCold-I to generate plasmid pJT026. The *invA3* cDNA was cloned into the *Nhe*I and *Bam*HI sites of expression vector pRSETb to create plasmid pJB063.

Construction of Chimeric Genes

The codon-optimized version of gene *invA3* was inserted into the *Nhe*I and *Bam*HI sites of expression vector pET28b to create plasmid pJB059. Subsequently, the portion of pJB059 encoding the TE domain of InvA3 was replaced by the corresponding portion of InvA5 (taken from plasmid pJB051) using the *Kpn*I and *Bam*HI restriction sites. The created chimeric gene *invA335* was cloned into expression vector pRSETb to create pJB074. It encodes a chimeric synthetase composed of the InvA3 adenylation-thiolation (A-T) didomain and the InvA5 thioesterase (TE) domain. A gene for the inverse chimera (InvA553, InvA5 A-T didomain fused to the InvA3 TE domain) was constructed using the Gibson Assembly Master Mix (New England Biolabs) using plasmids pJB051 and pJB059 as templates, to yield plasmid pJB075. The reactions (50 μl) consisted of 1.5–2.5 mM $MgCl_2$, 0.2 mM each dNTP, 20 pmol (each) primer (Table S1), and 1 U Phusion DNA polymerase in the supplied buffer and with the following thermocycling parameters, to create plasmid pJB075: 30 s at 98°C; 30 cycles of 98°C for 10 s, 48°C, 57°C, and 64.5°C, respectively, for 15 s, and 72°C for 45 s (InvA3 TE domain), 90 s (InvA5 A-T didomain), and 3 min (pET28b); and a terminal hold for 5 min at 72°C. To create the chimeric gene *invA556* (encoding the InvA5 A-T didomain fused to the InvA6 TE domain), plasmid pJB048 (*invA5*, cloned into pRSETb) was used. The gene portion encoding the TE domain of *invA6* was excised by *Cla*I and *Bam*HI restriction from pJB066 and ligated to pJB048, cut equally, to yield pJB071. The complete chimeric gene *invA556* was then cloned between the *Nde*I and *Bam*HI sites of pET28b, which yielded the final expression plasmid pJB072.

Heterologous Gene Expression and In Vitro Enzyme Characterization

N-Terminally hexahistidine-tagged InvA2, InvA4, InvA5, InvA553, InvA556, and PptA were produced in *E. coli* KRX, transformed with plasmids pJB053, pJB064, pJB051, pJB075, pJB072, and pJB062, respectively. Expression of genes *invA1*, *invA3*, *invA6*, and *invA335* was accomplished in *E. coli* SoluBL transformed with plasmids pJB078, pJB063, pJT026, and pJB074, respectively. For details on gene expression and protein purification, see Supplemental Experimental Procedures. To characterize the InvA1-A6 adenylation domains, the ATP-[^{32}P]pyrophosphate exchange assay was used as described by Schneider et al. (2008). 4-Hydroxyphenylpyruvate, or other substrates (Table S2) to determine substrate specificities, were added at 1 mM final concentration. To determine optima, the temperature was varied from 10°C to 35°C, and the pH from 6.0 to 8.2 with phosphate or Tris buffers, covering overlapping pH ranges.

In Vitro Biotransformation

Conversion of *apo*-enzymes into their *holo* form was catalyzed by the phosphopantetheinyl transferases Svp (Sanchez et al., 2001) or PptA. 0.5 μM of the respective *apo*-enzyme and 0.5 μM Svp or PptA were incubated for 30 min at 20°C–25°C in 75 mM Tris-HCl buffer (pH 6.8–7.6), and 120 μM coenzyme A as donor substrate. Product formation was accomplished in 500-μl reactions, containing 75 mM Tris-HCl buffer (pH 6.8–7.6, according to the optimum conditions), 5 mM $MgCl_2$, 125 nM EDTA, 2.5 mM ATP, 0.5 μM InvA, and 1.8 mM 4-hydroxyphenylpyruvic acid, at 20°C–25°C for 16 hr. The reaction mixtures were extracted twice with an equal volume of ethyl acetate, and the organic extract was concentrated under reduced pressure. For analytical HPLC (see below), the extracts were dissolved in methanol.

Synthesis of Deuterated Atromentin

The synthesis of deuterated 4-hydroxyphenylpyruvic acid was carried out according to a described method (Munde et al., 2013). The synthesis of

deuterated atromentin was carried out in analogy to the in vitro atromentin formation (see above). A reaction mixture (8 ml) consisted of 75 mM Tris-HCl buffer (pH 7.2), 10 mM $MgCl_2$, 125 nM EDTA, 5 mM ATP, 4 μM InvA1, 4 μM Svp, 114 μM coenzyme A, and 3 mM deuterated 4-hydroxyphenylpyruvic acid. It was incubated for 16 hr at 25°C and subsequently extracted three times with an equal volume of ethyl acetate. The extract was dissolved in methanol, and purification was accomplished by preparative HPLC (see below).

Stable-Isotope Labeling

For supplementation with stable-isotope-labeled atromentin, *P. involutus* was grown in Petri dishes on a layer of glass beads immersed in liquid medium (van Schöll et al., 2006). A monolayer of autoclaved 4-mm glass beads was poured into the bottom of a 9-cm Petri dish and 10 ml of MMN medium was added. A mycelial plug was cut from the mycelial margin of a culture actively growing on MMN agar and transferred to the center of the glass-bead plate. After 9 days of incubation at 18°C–20°C in the dark, the MMN medium was removed. The glass beads and the mycelium were washed with sterile MilliQ water, and 10 ml of MMN medium without a nitrogen source was added. After 24 hr, the mycelium was washed with sterile MilliQ water. Subsequently, 10 ml of maize hot extract supplemented with glucose (final concentration 2.5 g/l; pH 4) was added (Rineau et al., 2012; Shah et al., 2013). The culture was incubated for another 7 days at 18°C–20°C in the dark. For the first feeding experiment with homogenized mycelium, ten plates of *P. involutus* were cultivated as described above. The mycelium was then homogenized in 100 ml of 75 mM Tris-HCl buffer (pH 7.2) supplemented with 1 mM PMSF, using an Ultra-Turrax T25 basic (IKA). Unlabeled or 3′,3″,5′,5″-D_4-atromentin was added to 30 ml of homogenized mycelium at a final concentration of 1 mM. As control, another 30 ml was left without any labeled compounds. The reactions were incubated for 24 hr at room temperature and then extracted three times with 30 ml of ethyl acetate. The organic extracts were concentrated under reduced pressure. The extracts were redissolved in methanol for analytical HPLC (see below). For the second labeling experiment, six plates of *P. involutus* were cultivated as described above. Two plates were supplemented with 3′,3″,5′,5″-D_4-atromentin (final concentration: 1.5 mM, added together with the maize hot extract). Another two plates without labeled compounds served as control. The cultures were incubated for another 7 days at 18°C–20°C in the dark, before the media were extracted three times with ethyl acetate and further processed as described above.

Chromatography and Mass Spectrometry

HPLC analysis of in vitro product formation was performed on an Agilent 1200 system equipped with a Zorbax Eclipse XDB-C_{18} column (4.6 × 150 mm, 5 μm particle size). Solvent A was 0.1% (v/v) trifluoroacetic acid in water, and solvent B was methanol. The solvent gradient was: initial hold at 5% B, for 0.5 min, linear gradient from 5% to 90% B within 14.5 min, held at 90% B for 2 min, increased to 100% B within 0.5 min, and held for 4.5 min, at a flow rate of 1.0 ml/min. The detection wavelength range was 200–600 nm; chromatograms were extracted at λ = 254 nm. HPLC to analyze compounds after stable-isotope feeding was carried out as described above, but using a Nucleosil 100-5 C_{18} column (4.6 × 250 mm, 5 μm particle size) and the following gradient: initial hold at 5% B for 10 min, linear gradient 5%–50% B within 60 min, then increased to 100% B within 10 min, then held for another 5 min, at a flow rate of 1.0 ml/min.

High-resolution mass spectra were recorded on an Exactive Orbitrap mass spectrometer (Thermo) in the negative mode using electrospray ionization and equipped with a Betasil C_{18} column (Thermo, 2.1 × 150 mm; 3 μm particle size). Solvent A was 0.1% (v/v) formic acid in water, and solvent B was 0.1% (v/v) formic acid in acetonitrile. The solvent gradient was: initial hold at 5% B, for 1 min, linear gradient from 5% to 98% B within 15 min, then held at 98% B for 3 min, at a flow rate of 0.2 ml/min.

Preparative HPLC to purify deuterated atromentin was performed on an Agilent 1260 Infinity System, equipped with a Zorbax Eclipse XBD-C_8 column (21.2 × 250 mm; 7 μm particle size), at a flow rate of 25 ml/min. Solvent A was 0.1% (v/v) trifluoroacetic acid in water, and solvent B was acetonitrile. The gradient was: linear increase from 5% to 80% B within 20 min, increased to 100% in 1 min, and held for another 1 min. The detection wavelength range was λ = 200–600 nm.

Transcriptomic Analysis

Fungal mycelia were grown as described above, but using BSA (16% [w/w] N) as sole nitrogen source, or organic matter extracts (forest hot extract, maize hot extract, and maize compost). For each treatment there were three biological replicates with three Petri dishes per replicate. The biomass was collected and immediately dropped into a clean mortar filled with liquid nitrogen, and homogenized using a pestle. Total RNA was isolated using the RNeasy Plant Mini Kit (Qiagen) with the RLC buffer and the on-column DNase treatment according to the manufacturer. Total RNA was eluted in diethylpyrocarbonate-treated H_2O and stored at −20°C until use. For quality assessments, all samples were inspected using an RNA 6000 Nano kit on an Agilent 2100 Bioanalyzer. The microarray analysis was performed using already published data including six biological replicates on the reference MMN medium that are available at NCBI GEO (accession numbers NCBI-GEO: GSM848412–GSM848414 and GSM848421–GSM848423), as well as three replicates each for forest hot extract (GSM848415–GSM848417), maize hot extract (GSM848418–GSM848420), maize compost (GSM848424–GSM84842), and BSA (GSE47838) (Rineau et al., 2012; Shah et al., 2013).

SUPPLEMENTAL INFORMATION

Supplemental Information includes Supplemental Experimental Procedures, two figures, and two tables and can be found with this article online at http://dx.doi.org/10.1016/j.chembiol.2015.08.016.

AUTHOR CONTRIBUTIONS

J.B. performed molecular biological and biochemical experiments and chromatographic analyses; S.G. synthesized gyrocyanin; F.S. and A.T. generated and interpreted the transcriptomic data; D. Heine provided critical input on the synthesis of deuterated atromentin; J.T. cloned and expressed the *invA6* gene; D. Hoffmeister designed the study and co-wrote the paper together with C.H., P.S., and A.T.

ACKNOWLEDGMENTS

This work was supported by the Deutsche Forschungsgemeinschaft (DFG grant HO2515/4-1 to D. Hoffmeister). A stipend of the Studienstiftung des deutschen Volkes to D. Heine is gratefully acknowledged. P.S. is grateful to the Daimler und Benz Stiftung for a Research Scholarship, and J. T. acknowledges funding by the Collaborative Research Center ChemBioSys (SFB1127/1). We thank Andrea Perner and Heike Heinecke (Leibniz Institute for Natural Product Research and Infection Biology, Hans Knöll Institute, Jena, Germany) for recording mass and NMR spectra, respectively.

Received: June 7, 2015
Revised: August 17, 2015
Accepted: August 27, 2015
Published: October 22, 2015

REFERENCES

Besl, H., Bresinsky, A., Steglich, W., and Zipfel, K. (1973). Pilzpigmente XVII. Über Gyrocyanin, das blauende Prinzip des Kornblumenröhrlings (*Gyroporus cyanescens*) und eine oxidative Ringverengung des Atromentins. Chem. Ber. *106*, 3223–3229.

Besl, H., Bresinsky, A., Herrmann, R., and Steglich, W. (1980). Chamonixin and involutin, two chemosystematically interesting cyclopentanediones from *Gyrodon lividus*. Z. Naturforsch. *35C*, 824–825.

Biggins, J.B., Liu, X., Feng, Z., and Brady, S.F. (2011). Metabolites from the induced expression of cryptic single operons found in the genome of *Burkholderia pseudomallei*. J. Am. Chem. Soc. *133*, 1638–1641.

Bresinsky, A. (1974). Zur Frage der taxonomischen Relevanz chemischer Merkmale bei Hoeheren Pilzen. Bull. Soc. Linnéenne Lyon, 61–84.

Bresinsky, A., and Rennschmidt, A. (1971). Pigmentmerkmale, Organisationsstufen und systematische Gruppen bei höheren Pilzen. Ber. Dtsch. Bot. Ges. *84*, 313–329.

Bruner, S.D., Weber, T., Kohli, R.M., Schwarzer, D., Marahiel, M.A., Walsh, C.T., and Stubbs, M.T. (2002). Structural basis for the cyclization of the lipopeptide antibiotic surfactin by the thioesterase domain SrfTE. Structure *10*, 301–310.

Cantu, D.C., Chen, Y., and Reilly, P.J. (2010). Thioesterases: a new perspective based on their primary and tertiary structures. Protein Sci. *19*, 1281–1295.

Conti, E., and Izaurralde, E. (2005). Nonsense-mediated mRNA decay: molecular insights and mechanistic variations across species. Curr. Opin. Cell Biol. *17*, 316–325.

Eastwood, D.C., Floudas, D., Binder, M., Majcherczyk, A., Schneider, P., Aerts, A., Asiegbu, F.O., Baker, S.E., Barry, K., Bendiksby, M., et al. (2011). The plant cell wall-decomposing machinery underlies the functional diversity of forest fungi. Science *333*, 762–765.

Edwards, R.L., and Gill, M. (1973). Constituents of the higher fungi. Part XII. Identification of involutin as (-)-cis-5-(3,4-dihydroxyphenyl)-3,4-dihydroxy-2-(4-hydroxyphenyl)-cyclopent-2-enone and synthesis of (±)-cis-involutin trimethyl ether from isoxerocomic acid derivates. J. Chem. Soc. (London) Perkin Trans. I, 1529–1537.

Edwards, R.L., Elsworthy, G.C., and Kale, N. (1967). Constituents of higher fungi. Part IV. Involutin, a diphenyl-cyclopenteneone from *Paxillus involutus* (Oeder ex Fries). J. Chem. Soc. C, 405–409.

Forseth, R.R., Amaike, S., Schwenk, D., Affeldt, K.J., Hoffmeister, D., Schroeder, F.C., and Keller, N.P. (2013). Homologous NRPS-like gene clusters mediate redundant small-molecule biosynthesis in *Aspergillus flavus*. Angew. Chem. Int. Ed. Engl. *52*, 1590–1594.

Gill, M., and Steglich, W. (1987). Pigments of fungi (Macromycetes). Fortschr. Chem. Org. Naturst. *51*, 1–317.

Gruber, G., Kerschensteiner, L., and Steglich, W. (2014). Chromapedic acid, pulvinic acids and acetophenone derivatives from the mushroom *Leccinum chromapes* (Boletales). Z. Naturforsch. *69B*, 432–438.

Hermann, R. (1980). Untersuchungen zur Konstitution, Synthese und Biosynthese von Pilzfarbstoffen (Germany: Rheinische Friedrich-Wilhelms-Universität Bonn), doctoral thesis.

Hoyer, K.M., Mahlert, C., and Marahiel, M.A. (2007). The iterative gramicidin S thioesterase catalyzes peptide ligation and cyclization. Chem. Biol. *14*, 13–22.

Keszenman-Pereyra, D., Lawrence, S., Twfieg, M.E., Price, J., and Turner, G. (2003). The npgA/cfwA gene encodes a putative 4'-phosphopantetheinyl transferase which is essential for penicillin biosynthesis in *Aspergillus nidulans*. Curr. Genet. *43*, 186–190.

Kohler, A., Kuo, A., Nagy, L.G., Morin, E., Barry, K.W., Buscot, F., Canbäck, B., Choi, C., Cichocki, N., Clum, A., et al. (2015). Convergent losses of decay mechanisms and rapid turnover of symbiosis genes in mycorrhizal mutualists. Nat. Genet. *47*, 410–415.

Larrondo, L.F., Gonzalez, B., Cullen, D., and Vicuna, R. (2004). Characterization of a multicopper oxidase gene cluster in *Phanerochaete chrysosporium* and evidence of altered splicing of the mco transcripts. Microbiology *150*, 2775–2783.

Lindahl, B.D., and Tunlid, A. (2015). Ectomycorrhizal fungi—potential organic matter decomposers, yet not saprotrophs. New Phytol. *205*, 1443–1447.

Misiek, M., and Hoffmeister, D. (2008). Processing sites involved in intron splicing of Armillaria natural product genes. Mycol. Res. *112*, 216–224.

Munde, T., Brand, S., Hidalgo, W., Maddula, R.K., Svatos, A., and Schneider, B. (2013). Biosynthesis of tetraoxygenated phenylphenalenones in *Wachendorfia thyrsiflora*. Phytochemistry *91*, 165–176.

Rineau, F., Roth, D., Shah, F., Smits, M., Johansson, T., Canbäck, B., Olsen, P.B., Persson, P., Grell, M.N., Lindquist, E., et al. (2012). The ectomycorrhizal fungus *Paxillus involutus* converts organic matter in plant litter using a trimmed brown-rot mechanism involving Fenton chemistry. Environ. Microbiol. *14*, 1477–1487.

Samel, S.A., Wagner, B., Marahiel, M.A., and Essen, L.O. (2006). The thioesterase domain of the fengycin biosynthesis cluster: a structural base for the macrocyclization of a non-ribosomal lipopeptide. J. Mol. Biol. *359*, 876–889.

Sanchez, C., Du, L., Edwards, D.J., Toney, M.D., and Shen, B. (2001). Cloning and characterization of a phosphopantetheinyl transferase from *Streptomyces verticillus* ATCC15003, the producer of the hybrid peptide-polyketide antitumor drug bleomycin. Chem. Biol. *8*, 725–738.

Schneider, P., Weber, M., Rosenberger, K., and Hoffmeister, D. (2007). A one-pot chemoenzymatic synthesis for the universal precursor of antidiabetes and antiviral bis-indolylquinones. Chem. Biol. *14*, 635–644.

Schneider, P., Bouhired, S., and Hoffmeister, D. (2008). Characterization of the atromentin biosynthesis genes and enzymes in the homobasidiomycete *Tapinella panuoides*. Fungal Genet. Biol. *45*, 1487–1496.

Schwarzer, D., Finking, R., and Marahiel, M.A. (2003). Nonribosomal peptides: from genes to products. Nat. Prod. Rep. *20*, 275–287.

Shah, F. (2014). Insights into the Molecular Mechanisms of Litter Decomposition and Assimilation of Nitrogen by Ectomycorrhizal Fungi (Sweden: Lund University), Doctoral thesis. Lund University Publications, ISBN:978-91-7473-938-1.

Shah, F., Rineau, F., Canbäck, B., Johansson, T., and Tunlid, A. (2013). The molecular components of the extracellular protein-degradation pathways of the ectomycorrhizal fungus *Paxillus involutus*. New Phytol. *200*, 875–887.

Stachelhaus, T., Mootz, H.D., and Marahiel, M.A. (1999). The specificity conferring code of adenylation domains in nonribosomal peptide synthetases. Chem. Biol. *6*, 493–505.

Steglich, W., Steffan, K., Besl, H., and Bresinsky, A. (1977). Pilzpigmente 29. 2,5-Diarylcyclopentan-1,3-dione aus *Chamonixia caespitosa* (Basidiomycetes). Z. Naturforsch. *32c*, 46–48.

Trauger, J.W., Kohli, R.M., Mootz, H.D., Marahiel, M.A., and Walsh, C.T. (2000). Peptide cyclization catalysed by the thioesterase domain of tyrocidine synthetase. Nature *407*, 215–218.

van Schöll, L., Hoffland, E., and van Breemen, N. (2006). Organic anion exudation by ectomycorrhizal fungi and *Pinus sylvestris* in response to nutrient deficiencies. New Phytol. *170*, 153–163.

Wackler, B., Schneider, P., Jacobs, J.M., Pauly, J., Allen, C., Nett, M., and Hoffmeister, D. (2011). Ralfuranone biosynthesis in *Ralstonia solanacearum* suggests functional divergence in the quinone synthetase family of enzymes. Chem. Biol. *18*, 354–360.

Wackler, B., Lackner, G., Chooi, Y.H., and Hoffmeister, D. (2012). Characterization of the *Suillus grevillei* quinone synthetase GreA supports a nonribosomal code for aromatic α-keto acids. Chembiochem *13*, 1798–1804.

Wallander, H., and Söderström, B. (1999). Paxillus. In Ectomycorrhizal Fungi: Key Genera in Profile, J.W.G. Cairney and S.M. Chambers, eds. (Springer-Verlag), pp. 231–252.

Yeh, H.H., Chiang, Y.M., Entwistle, R., Ahuja, M., Lee, K.H., Bruno, K.S., Wu, T.K., Oakley, B.R., and Wang, C.C. (2012). Molecular genetic analysis reveals that a nonribosomal peptide synthetase-like (NRPS-like) gene in *Aspergillus nidulans* is responsible for microperfuranone biosynthesis. Appl. Microbiol. Biotechnol. *96*, 739–748.

Zeiler, E., List, A., Alte, F., Gersch, M., Wachtel, R., Poreba, M., Drag, M., Groll, M., and Sieber, S.A. (2013). Structural and functional insights into caseinolytic proteases reveal an unprecedented regulation principle of their catalytic triad. Proc. Natl. Acad. Sci. USA *110*, 11302–11307.

Zhou, Z.Y., and Liu, J.K. (2010). Pigments of fungi (Macromycetes). Nat. Prod. Rep. *27*, 1531–1570.

Zhu, J., Chen, W., Li, Y.Y., Deng, J.J., Zhu, D.Y., Duan, J., Liu, Y., Shi, G.Y., Xie, C., Wang, H.X., and Shen, Y.M. (2014). Identification and catalytic characterization of a nonribosomal peptide synthetase-like (NRPS-like) enzyme involved in the biosynthesis of echosides from *Streptomyces* sp. LZ35. Gene *546*, 352–358.

